Journal of Molecular Liquids 458 (2026) 129750

Contents lists available at ScienceDirect

Journal of Molecular Liquids

journal homepage: www.elsevier.com/locate/molliq

Chemical speciation of Co^{2+} and Ni^{2+} ions in deep eutectic solvents and highly efficient colorimetric determination of cobalt from lithium-ion battery samples using UV/Vis

Ali Iname [a,b], Véronique Vitry [a], Issa Tapsoba [b,*]

[a] Metallurgy Department, University of Mons, Faculty of Engineering, 56 Rue de l'Epargne, 7000 Mons, Belgium
[b] Laboratory of Analytical, Environmental and Bio-Organic Chemistry (LCAEBIO), Joseph KI-Zerbo University, Chemistry Department of 03 BP 7021 Ouagadougou 03, Burkina Faso

ARTICLE INFO

Keywords:
Speciation
Deep eutectic solvents
Hydrogen bond donors
Nickel
Cobalt
Colorimetric determination

ABSTRACT

In this work, deep eutectic solvents (DESs) based on choline chloride combined with various hydrogen bond donors (HBDs), namely choline chloride-lactic acid (1:2), choline chloride-malonic acid (1:1), choline chloride-glycerol (1:2), choline chloride-ethylene glycol (1:2) and choline chloride-urea (1:2) were prepared and characterized. These DESs were used to investigate the chemical speciation of Co^{2+} and Ni^{2+} metal ions by Uv-visible spectrophotometry, exploiting the characteristic coloration of the solutions.

The colorimetric determination of Co^{2+} in lithium-ion battery cathode samples was carried out using the choline chloride-lactic acid (1:2) DES.

The results showed that Co^{2+} preferentially forms tetrachlorocobaltate (II) complexes, $[CoCl_4]^{2-}$, in all DESs systems studied, corresponding to a tetrahedral geometry stabilized by the chloride ions coordination. In contrast, Ni^{2+} ions exhibit a ligand dependent dual speciation on the ligand strength. In DESs containing weak-field ligands, such as chloride with lactic acid, glycerol, ethylene glycol or urea, octahedral Ni^{2+} species dominate, including solvated complexes of the type $[NiCl_x(HBD)_{6-x}]^{4-x}$. When the DES contains a stronger-field ligand, such as malonate, Ni^{2+} preferentially forms the tetrahedral tetrachloronickelate (II) complexes $[NiCl_4]^{2-}$. These results demonstrate that the nature of the hydrogen bond donor strongly influences the coordination environment and speciation of Ni^{2+} in deep eutectic solvent media.

For the colorimetric determination of cobalt in the cathode samples, the analysis of three samples yielded concentrated of 56 ± 0.7 mg L^{-1}; 46.48 ± 0.7 mg L^{-1} and 47.17 ± 2 mg L^{-1}. These values were confirmed by inductively coupled plasma optical emission spectrometry (ICP-OES) results, thus proving the methods accurate.

1. Introduction

The growing development and use of Li-ion batteries for green technologies, such as electric vehicles, wind turbines and solar cells, contribute to the fight against global warming [1]. However, the sustainability of these technologies depends deeply on the availability of the raw materials used in the manufacture of Li-ion batteries such as cobalt, nickel, and lithium [2,3].

These metals are considered critical and/or strategic due to their potentially limited supply in the long term [4,5]. In addition, it is well known that conventional extraction, such as pyrometallurgy and/or hydrometallurgy, often uses aggressive and toxic chemical solutions [3,6,7].

In this context, the recovery and recycling of these metals appears to be essential for promoting the circular economy and reducing dependence on primary mining.

For sustainable development, metal separation and recovery processes must adhere to the principles of green chemistry, particularly using environmentally friendly solvents. A promising alternative such as ionic liquids (ILs) and deep eutectic solvents (DESs) was used [1,2,7]. Ionic liquids have demonstrated their effectiveness in the separation of strategic metals such as nickel and cobalt [8]. However, their complex synthesis and purification significantly increase the cost of the process.

Deep eutectic solvents (DESs), on the other hand, offer several advantages. Indeed, they are generally composed of inexpensive and available reagents, such as choline chloride, carboxylic acids like oxalic

* Corresponding author.
E-mail address: issa.tapsoba@ujkz.bf (I. Tapsoba).

https://doi.org/10.1016/j.molliq.2026.129750
Received 24 March 2026; Received in revised form 14 June 2026; Accepted 16 June 2026
Available online 27 June 2026

acid, malonic acid, lactic acid; glycerol; urea and ethylene glycol. They are also less toxic and more biodegradable than ionic liquids [6,7,9–12]. Carboxylic acid-based DESs are particularly attractive for metal leaching due to their strong solubilizing power, linked to the ability of acid to act as good oxygen acceptors [1,13].

To make these green solvents usable on an industrial scale, particularly for the extraction and selective separation of metals, it is essential to have reliable methods for measuring metal ions. Among the available techniques, inductively coupled plasma optical spectroscopy (ICP-OES), X-ray fluorescence (XRF), or atomic absorption spectroscopy (AAS) are the most common. However, these techniques often require significant dilutions which can lead to significant analytical errors. In addition, DES have higher viscosity than water and a high organic carbon content, making direct analyses by ICP-OES difficult without pretreatment [14–16].

In this context, UV–Visible spectroscopy is an interesting alternative due to its low cost and simplicity. UV–Vis is based on the measurement of the absorbance of a colored metal complex, allowing the quantitative determination of concentration. It was reported in the literature that most existing colorimetric methods have been developed in aqueous media. It is therefore necessary to investigate them in deep eutectic solvents, to allow their reliable and reproducible use.

To our knowledge, very few studies have been carried out on the in-depth study of the chemical speciation of Co^{2+} and Ni^{2+} ions in deep eutectic solvents [1,9,17,18]. In addition, no in-depth study has yet been published on the colorimetric determination of metal ions, in particular Co^{2+} and Ni^{2+} ions, in deep eutectic solvents. In order to contribute to the development of green and sustainable recycling methods for critical and/or strategic metals contained in Li-ion batteries, the present work aims to advance the understanding of Co^{2+} and Ni^{2+} ions speciation in DESs and to establish a reliable UV–visible spectrophotometry method for their colorimetric determination in such media. The chemical speciation of these metals in different deep eutectic solvents has been investigated by UV/vis and Fourier transform infrared (FTIR) spectroscopies.

2. Experimental

2.1. Reagents and equipment

The compounds used in this work, namely choline chloride, lactic acid, glycerol, urea and, cobalt chloride hexahydrate ($CoCl_2$,$6H_2O$), nickel chloride hexahydrate ($NiCl_2$,$6H_2O$), were purchased from VWR and used without further purification. Malonic acid and ethylene glycol were purchased from Merck and used without further purification. Lithium Cobalt oxide ($LiCoO_2$) powder (particle size 0.5 μm) was purchased from Merck and used as received. The detailed characteristics of chemicals used are summarized in Table 1.

Table 1
Chemical specifications.

Reagents	Molar mass (g. mol^{-1})	Raw formula	CAS number	Purity	supplier
Choline chloride	139.62	$C_5H_{14}ClNO$	67–48-1	≥ 98%	
Lactic acid	90.08	$C_3H_6O_3$	50–21-5	90%	
Glycerol	92.09	$C_3H_8O_3$	56–81-5	97%	
Urea	60.06	CH_4N_2O	57–13-6	99.7%	VWR
Cobalt chloride hexahydrate	237.93	$CoCl_2.6H_2O$	7791-13-1	98.3%	
Malonic acid	104.06	$C_3H_4O_4$	141–82-2	99%	
Ethylene glycol	62.07	$C_2H_6O_2$	107–21-1	99.5%	Merck
Lithium cobalt oxide	97.87	$LiCoO_2$	12,190–79-3	99.5%	

2.2. Deep eutectic solvents (DESs) preparation and metal salt leaching

For the preparation of type III deep eutectic solvents, the quaternary ammonium salt hydrogen bond acceptor (HBA) choline chloride (ChCl) was combined with hydrogen bond donors (HBD) such as lactic acid (monocarboxylic acid), malonic acid (dicarboxylic acid), glycerol (alcohol), ethylene glycol(alcohol) and urea (diamide) according to the literature [10,19].The chemical structure of its compounds is shown in fig. S1.

For each DES, choline chloride was mixed with hydrogen bond donors (HBD) at 1:2 M ratio for choline chloride-lactic acid, choline chloride-glycerol, choline chloride-ethylene glycol and choline chloride-urea or 1:1 M ratio for choline chloride malonic acid. These hydrogen bond donors (HBD) were selected due to their different physicochemical, as previously reported in the literature [10,19–24]. The Choline chloride (ChCl) based DESs, together with their compositions and properties, are presented in the Table 2.

These DESs were prepared according to their molar ratios already well established in the literature [10,19].

The preparation was carried out in borosilicate glass at a moderate temperature of 80 °C, stirred (400 rpm) until an homogenous and colorless liquid was formed over a period of 2 h.

The prepared solvents, with characteristics reported previously [22,25–28], were used without prior characterization.

Solutions of various concentrations (mmol Kg^{-1}) of $NiCl_2.6H_2O$ salts from 10 mmol Kg^{-1} to 50 mmol Kg^{-1} were made by adding the required amount of metal salts in choline chloride-lactic acid (1:2), choline chloride-glycerol (1:2), choline chloride-ethylene glycol (1:2) and choline chloride-urea(1:2) DESs at 80 °C and continuously stirring till full dissolution. In the DES of choline chloride malonic acid (1:1) various solutions of $NiCl_2.6H_2O$ salts were prepared from 1 mmol Kg^{-1} to 5 mmol Kg^{-1}.

For the $CoCl_2.6H_2O$ salts, solutions of various concentrations (mmol Kg^{-1}) of 0.2 mmol Kg^{-1} to 1 mmol Kg^{-1} were made by adding the required amount of metal salts in all DESs.

The masses of the metallic salts were determined using the following formula (1):

$$m_{(salts)} = 10^{-6}.C.M.m_{(DESs)} \quad (1)$$

where C is the salt concentration (mmol Kg^{-1}), M is the salt molar mass (g mol^{-1}) and m is the mass (g) of DES.

2.3. UV/Vis and FT-IR spectroscopy

UV–visible absorption spectra were recorded in the 280 to 780 nm range (spectral resolution 4 nm), using PerkinElmer (Lambda 365) spectrometer with software UV express Version 4.1.0. Around 3 mL of DES or metal solutions were placed in the analysis cell before direct measurement. A blank was then run to eliminate interfering signals for each solvent. The wavelength scanning range was determined for each solvent before experiments were run.

The calibration curve was obtained by plotting absorbance (A) as a function of Co^{2+} concentration (C), following the Beer Lambert relationship (eq. 2).

$$A = \varepsilon_\lambda.l.C \quad (2)$$

where A is the absorbance, C the concentration of Co^{2+}, Ɛ specific molar extinction coefficient (L.mol^{-1}.cm^{-1}) and l tank thickness (1 cm).

IR spectra were recorded in wave range of 400–4000 cm^{-1}, with a spectral resolution of 4 cm^{-1}, using a Fourier transform spectrometer (Shimadzu FTIR-8400S). The data were collected using IR solution software.

The viscosity of the DESs was determined using an Anton Paar MCR

Table 2
Choline chloride (ChCl) based DESs and their compositions and properties.

Hydrogen Bond Acceptor (HBA)	Hydrogen Bond Donors (HBDs)	Molar ratio (ChCl:HBDs)	Abbreviation	Melting point (°C)	Density ($g.cm^{-3}$)	Viscosity (mPa.s)
Choline chloride (ChCl)	Lactic acid	1:2	ChCl-Lac	−46	1.16	42(30 °C)
	Glycerol		ChCl-Gly	−40	1.18	259(25 °C)
	Ethylene glycol		ChCl-EG	−66	1.11	44.4(25 °C)
	Urea		ChCl-Ur	12	11.979	750(25 °C)
	Malonic acid	1:1	ChCl-Malo	10	10.66	829(25 °C)

302 rheometer with a planar-planar geometry and a 1 mm gap. The results were collected using RheoCompass 1.19 software.

The pH and electrochemical potential (mV) were measured using a WTW 3110 instrument equipped with appropriate probes.

Three LCO Li-ion battery cathode samples (X3; X4 and X5) were dissolved in the DES choline chloride - lactic acid (1:2) at 80 °C for 12 h. For each sample, three analyses were performed to measure the cobalt absorbance and verify the repeatability of the measurements. The cobalt content was determined from eq. (2). Inductively coupled plasma optical spectroscopy (ICP-OES) (Perkin Elmer, 7300DV) was used to validate the colorimetric determination of Co^{2+} ions in deep eutectic solvents by using these same samples.

3. Results and discussion

3.1. Characterization of DESs

3.1.1. Analysis by Fourier transform spectrometer

Hydrogen bonds play a crucial role in the formation of deep eutectic solvents, whose structure relies on specific molecular interactions between their constituents [29]. To highlight these interactions and better understand the formation mechanism of DESs system, Fourier transform infrared (FTIR) spectroscopy analyses were performed on choline chloride, hydrogen bond donors (HBDs), and the corresponding eutectic mixture.

The FTIR spectra were superimposed to compare the characteristic bands of the different compounds. This approach allows for the identification of spectral modifications associated with functional groups involved in hydrogen bonding and provides information on the structure of the eutectic mixture. The results are presented in Fig. 1.

The FTIR spectrum of choline chloride (Fig. 1.a, black spectrum) exhibits several characteristic absorption bands. A broad band observed between approximately 3400 cm^{-1} and 3600 cm^{-1} is assigned to the O—H stretching vibration of the hydroxyl group present in the choline cation. Another prominent band located around 1475 cm^{-1} corresponds to the symmetric bending vibration associated with the quaternary ammonium group ($N^{+}(CH_3)_3$), and the C—N bond vibrations characteristic of choline chloride [9,30].

The FTIR spectrum of lactic acid (Fig. 1a, red spectrum) is characterized by a broad absorption band extending from approximately 2500 to 3400 cm^{-1}, attributed to the O—H stretching vibration of the carboxylic acid group involved in extensive hydrogen bonding. An intense absorption band centered near 1710 cm^{-1} is assigned to the C═O stretching vibration of the carboxylic acid carbonyl group [3,9,32].

Upon mixing choline chloride and lactic acid to form the deep eutectic solvent (DES), significant spectral changes are observed in the FTIR spectrum (Fig. 1a, blue spectrum). In particular, the broad O—H stretching band becomes wider and shifts toward lower wavenumbers. This bathochromic shift is indicative of stronger hydrogen-bonding interactions and reflects the formation of an extended intermolecular

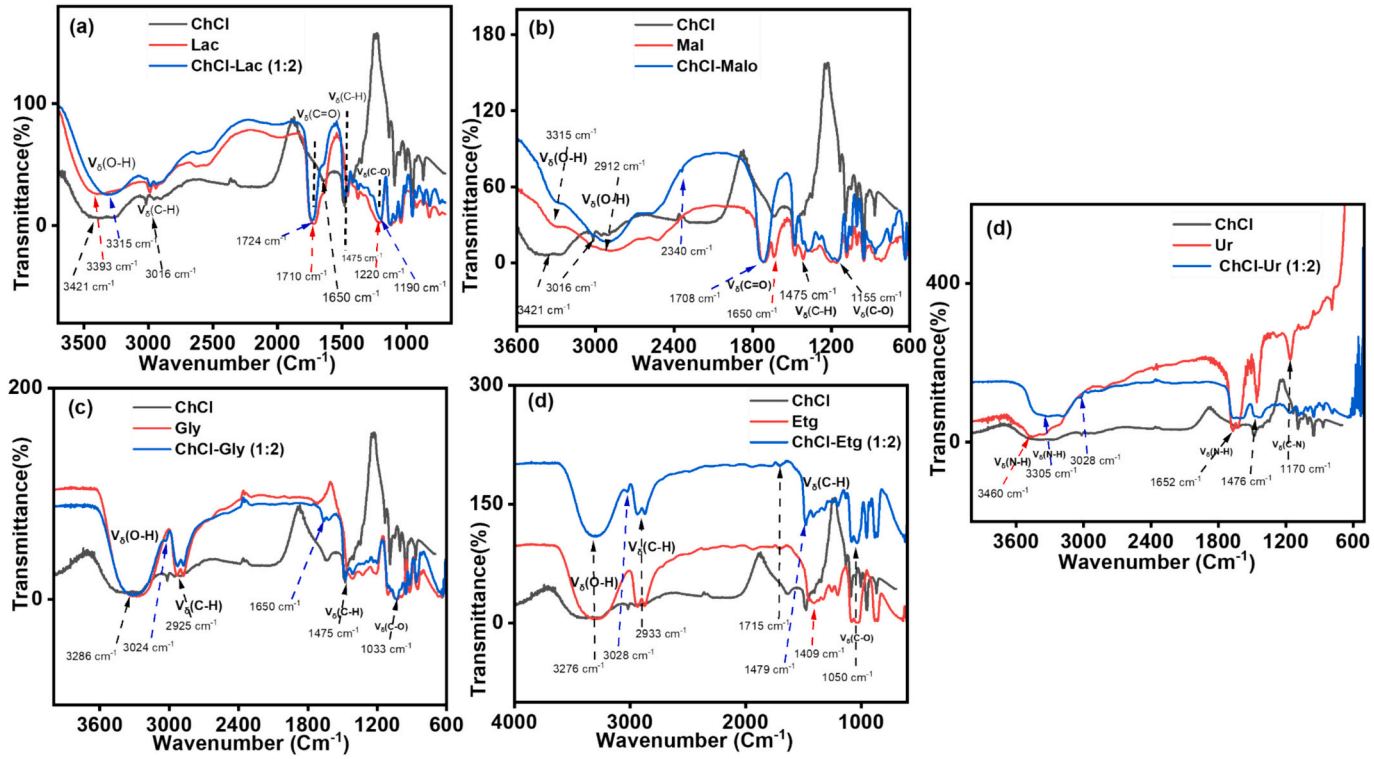

Fig. 1. FT-IR spectra (4000 cm^{-1} - 650 cm^{-1}) ChCl, HDB and DESs: (a) ChCl-Lac (1:2); (b) ChCl-Malo (1:1); (c) ChCl-Gly (1:2); (d) ChCl-EG (1:2) and ChCl-Ur (1:2).

hydrogen-bond network between choline chloride and lactic acid molecules during DES formation [9].

Additional evidence for DES formation is provided by the shifts observed in other characteristic vibrational bands. The O—H stretching band shifts from 3421 cm^{-1} in choline chloride and 33,963 cm^{-1} in lactic acid to 3315 cm^{-1} in the DES, confirming the involvement of hydroxyl groups in hydrogen-bond formation. Similarly, the carbonyl stretching vibration undergoes a shift from 1710 cm^{-1} in pure lactic acid to 1724 cm^{-1} in the DES. This variation reflects changes in the electronic environment of the carbonyl group resulting from its participation in intermolecular interactions with the chloride anion and hydroxyl groups of choline chloride [9,28,31]. Furthermore, the C—O stretching vibration shifts from 1220 cm^{-1} in lactic acid to 1190 cm^{-1} in the eutectic mixture, providing additional evidence of hydrogen-bond-mediated structural reorganization.

These spectral modifications demonstrate that the interactions present in the DES differ significantly from those in the pure components. The observed band shifts and broadening indicate the replacement of the original hydrogen-bonding environment by a new and more extensive intermolecular hydrogen-bond network involving chloride choline and lactic acid molecules.

Based on these spectroscopic observations, a mechanism for the formation of the ChCl–Lac (1:2) deep eutectic solvent is proposed (Fig. 2). The mechanism is primarily governed by the establishment of strong intermolecular hydrogen-bonding interactions between the chloride anion and the hydroxyl and carboxyl functional groups of lactic acid, resulting in the formation of a stable eutectic liquid structure.

The spectral changes observed during the preparation of DES ChCl-Lac (1:2) (Fig. 1a) are also evident for DESs ChCl-Malo (1:2) (Fig. 1b), ChCl-Gly (1:2) (Fig. 1c), ChCl-EG (1:2) (Fig. 1d), and ChCl-Ur (1:2) (Fig. 1e). These changes confirm the establishment of specific interactions between the constituents of the different DESs studied. All the results obtained are summarized in Table 3.

The infrared spectrum obtained for DES ChCl-Malo (1:1) is in good agreement with that reported in the literature [2]. Similarly, the FTIR spectra recorded for DESs ChCl-Gly (1:2) and ChCl-EG (1:2) show similar characteristics, and the observed spectra are also consistent with those in the literature [27,33,34].

The observed shifts in characteristic absorption bands, the appearance of new bands, and the variations in band in band intensities indicate the establishment of extensive hydrogen bonding interactions between choline chloride and the hydrogen bond donor. The spectral modifications are characteristic of a deep eutectic solvent formation.

Furthermore, the results obtained for the DES ChCl-Urea (1:2) are also consistent with those reported in the literature [25–27,34]. The main bands observed and their variations compared to the pure precursors confirm the presence of strong intermolecular interactions, leading to DES formation.

Overall, the FTIR characterization results provide clear evidence for the successful synthesis of all the DESs investigated.

To further assess their physicochemical properties, viscosity measurements were first performed, followed by the determination of electrochemical potential and pH. These parameters provide valuable information on the transport properties, ionic environment, and chemical behavior of the DESs [28].

Table 3
Characteristic band assignments of the FTIR for HBA, HBD and DESs.

HDB and DESs		Wave number (Cm^{-1})	Intensity	Functional groups
	HBD	DESs		
	3393	3315	Large, strong	O-H
HBD: Lactic acid	1710	1724	strong	C=O
DES: ChCl-Lac (1:2)	2980	2980	low	C-H
	1475	1475	medium	C-H (CH_2)
	1220	1190	medium	C-O
	2912–3315	2912–3315	Large, strong	O-H
	–	3240	Low	O-H
HBD: Malonic acid	1708	1708	strong	C-H
DES:ChCl-Malo (1:2)	1650	–	medium	C=O
	1475	1475	medium	C-H
	1155	1155	medium	C-O
	3286	3286	Large, strong	O-H
	–	3024	low	O-H
HBD: Glycerol	2925	2925	medium	C-H(CH_3)
DES: ChCl-Gly (1:2)	–	1650	medium	–
	1475	1475	medium	C-H (CH_2)
	1033	1033	low	C-C-O
	3276	3286	Large, strong	O-H
	–	3028	low	O-H
HBD: Ethylen glycol	2933	2933	medium	C-H(CH_3)
DES: ChCl-EG (1:2)	–	1715	medium	–
	1479	1479	medium	C-H (CH_2)
	1050	1050	low	C-C-O
	3460	3305	Large, strong	NH_2
HBD: Urea	–	3028	low	NH_2
DES: ChCl-Ur (1:2)	1652	1652	strong	N-H (NH_2)
	1476	1476	medium	C-H (CH_2)
	1170	1170	medium	C-N

3.1.2. *Study of the viscosity and potential of DESs*

The viscosity of the DES was measured at their preparation temperature (80 °C). Subsequently, their ionic conductivity and pH were determined at room temperature. The results are obtained in Table 4.

The results show that, at 80 °C, DES ChCl-Malo (1:2) exhibits the highest viscosity, followed by DES ChCl-Urea (1:2) and ChCl-Gly (1:2), with respective values of 101.5 mPa.s, 37.6 mPa.s, 32.7 mPa.s. The least viscous DESs are ChCl-EG (1:2) and ChCl-Lac (1:2), whose viscisities are 8.2 mPa.s and 16.5 mPa.s respectively. These results are in agreement with those reported in the literature [26,30] and confirm the formation of the deep eutectic solvents investigated.

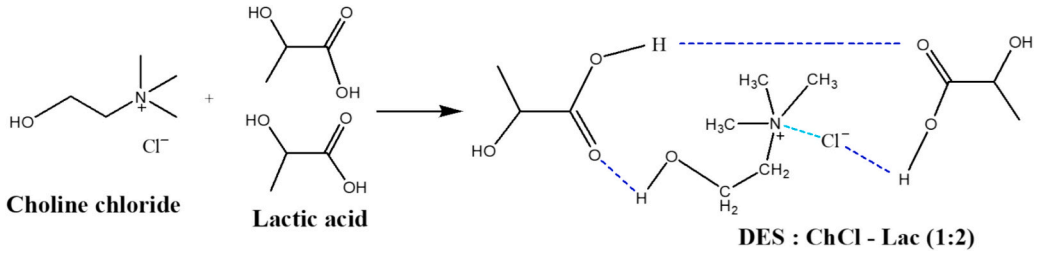

Fig. 2. Reaction scheme for the preparation of deep eutectic solvent.

Table 4
Study of the viscosity and conductivity of DESs.

DESs	Viscosity (mPa.s) at 80 °C	Potential (mV) at 25 °C	pH at 25 °C
ChCl-Lac (1:2)	**16.5**	**370.2**	**0.7**
ChCl-Gly (1:2)	**32.7**	**69.9**	**5.6**
ChCl-EG (1:2)	**8.2**	**32.8**	**6.2**
ChCl-Ur (1:2)	**37.6**	**92.2**	**8.2**
ChCl-Malo (1:2)	**101.5**	**474.2**	–

The electrochemical potential reveal that the DESs ChCl-Malo (1:2) and ChCl-Lac (1:2) exhibit the highest potentials, with respective values of 474.2 mV and 370.2 mV. The high potential observed could be attributed to their acidic character due to the presence of a high concentration of mobile ionic species in solution, particularly protons (H^+) in solution. This interpretation is supported by pH measurements, which confirm the acidic character of the ChCl-Malo (1:2) and ChCl-Lac (1:2) DESs. Indeed, DES ChCl-Lac (1:2) has a pH of 0.7. These results are in good agreement with literature data [24,28].

Conversely, DES ChCl-Urea (1:2) has the highest pH (8.2), reflecting a basic character. The DES ChCl-Gly (1:2) and ChCl-EG (1:2) have intermediate pH of 6.2 and 5.6, respectively.

Overall, these finding demonstrate that in the investigated DESs exhibit distinct physicochemical properties, which are expected to significantly influence their interactions with metallic species. Consequently, these DESs represent promising media for studying metallic salt speciation and metal-ligand interactions.

3.2. Spectroscopy study

3.2.1. UV/Vis spectroscopy spectra of pure nickel salts in DES

The UV/Vis spectra of $NiCl_2.6H_2O$ dissolved in the different DESs are shown on fig. S2.

These results show that Ni^{2+} ions exhibit the same coloration (green) in all deep eutectic solvents (DESs) used, except for the choline chloride-malonic acid DES, which displays a blue coloration.

Indeed, one can observe Fig.S2(a); Fig.S2(c); Fig.S2(d); Fig.S2(e) three characteristic absorption bands. A strong absorption band appears in the visible range (from 400 nm to 430 nm), accompanied by two weaker bands (from 685 nm to 760 nm). These results are summarized in Table 5.

In the case of the choline chloride-malonic acid (1:1) two intense absorption bands are located at 658.2 nm and 708.1 nm (Fig.S2. b). This difference may be attributed to the dicarboxylic nature of malonic acid (fig. S1). Indeed, it is reported in the literature that Ni^{2+} ions showed a blue coloration with dicarboxylic acids which bidentate ligands [1,2].

In addition, one can observe on fig. S2 that the intensity of absorption bands increases proportionally with the concentration of Ni^{2+} ions in the solution, without any shift in the characteristic wavelengths. This behavior is typical of a linear absorption process, consistent with the Beer-Lambert law (eq. 2) concluding that nickel ions amount could be determined using UV/Vis spectroscopy.

These results show that the nature of DES could affect considerably the speciation of nickel ions.

Table 5
Spectroscopic data from Ni^{2+} UV/Vis studies deep eutectic solvent with λ_{max}.

DESs	λmax /nm	Intensity	Figures
	425.3	strong	
ChCl - Lac (1:2)	708.3	low	Fig.S2(a)
	764.2	low	
	405.8	strong	
ChCl - Gly (1:2)	680	low	Fig.S2(c)
	746.7	low	
	420.9	strong	
ChCl – EG (1:2)	691.4	low	Fig.S2(d)
	760.5	low	
	417.8	strong	
ChCl - Ur (1:2)	680	low	Fig.S2(e)
	753.2	low	

3.2.2. UV/Vis spectroscopy spectra of pure cobalt salts in DES

The UV/Vis spectra of $CoCl_2.6H_2O$ dissolved in the different DESs are shown in Fig. S3.

The results indicate that, regardless of the eutectic solvent, the Co^{2+} ion exhibits four absorption bands respectively at 630 nm, 642 nm, 670 nm, and 697 nm, corresponding to a blue coloration.

These results are consistent with those reported by Amphlett et al, 2020 and correspond to the characteristic blue coloration observed in these systems, indicating similar coordination environments for cobalt across these DESs [1]. Comparatively to Ni^{2+} ions, these results showed that the DES does not affect the speciation of Co^{2+} ions.

Based on these preliminary results obtained for Ni^{2+} and Co^{2+} ions in DESs, the study of these ions in different DESs is essential to predict their solution behavior and to optimize the selectivity of metal dissolution and separation process within the framework of hydrometallurgy recycling of metals.

3.3. Cobalt and nickel speciation study

Metal speciation is a critical factor influencing the dissolution of metal salts and oxides and plays a central role in designing selective processes for metal separation and recovering [1,33].

A detailed investigation of cobalt and nickel speciation in these media provides interactions between metal ions and the various components of the DESs. These DESs are characterized by a high chloride anion content, which could serve as a potential ligand for metal complex formation as reported by Bučko et al, choline based DES contain approximately 5 mol L^{-1} of chloride anions, endowing the medium with significant complexation capacity toward metal cations [35].

In addition to chloride coordination, metal-ion speciation could be also influenced by the presence of molecules in DES, such as hydrogen bonds donors. In order to highlight the influence of the different molecules of DES in the speciation of Ni^{2+} and Co^{2+} ions, UV–visible spectroscopy was carried out on undiluted DES to preserve the native coordination environment of the metal ions [36].

3.3.1. Pure salts cobalt

At 80 °C, the following pure deep eutectic solvents: choline chloride-lactic acid (1:2), choline chloride-malonic acid (1:1), choline chloride-glycerol (1:2), choline chloride-ethylene glycol (1:2), and choline chloride-urea (1:2), are colorless. Upon dissolution of cobalt (II) chloride hexahydrate in these DESs, the resulting solutions display a blue color as illustrated in Fig. 3.

We can see in Fig.3. (b) the presence of absorptions bands of cobalt (II) ions from 400 nm to 780 nm. Therefore, the observed blue coloration indicates the formation of $[CoCl_4]^{2-}$ complex anion confirming that this specie predominates in the five choline-based DESs. This color is characterized by tetrahedral complexes $[CoCl_4]^{2-}$ [36]. These results are in agreement with reported literature [18,37] indicating that many common tetrahedral complexes present intense blue color.

Specifically, three intense bands appear around 630 nm, 670 nm and 695 nm (Fig.3.b) corresponding to spin-allowed $^4A_{2g}(F) \rightarrow {}^4T_{1g}(F)$ electronic transition, which is split into multiple components due to the ligand field [1,36]. This transition is both more intense and red-shifted, in agreement with observed blue coloration.

In the DES, cobalt (II) preferentially coordinates with chloride ions (Cl^-) over other molecules in the DES under the conditions studied. This preference is likely due to the high availability of Cl^- ions in solution compared to carboxylates leading to Co^{2+} and Cl^- coordination complex [35,38].

This may be explained by the fact that the chloride ion (Cl^-) is a

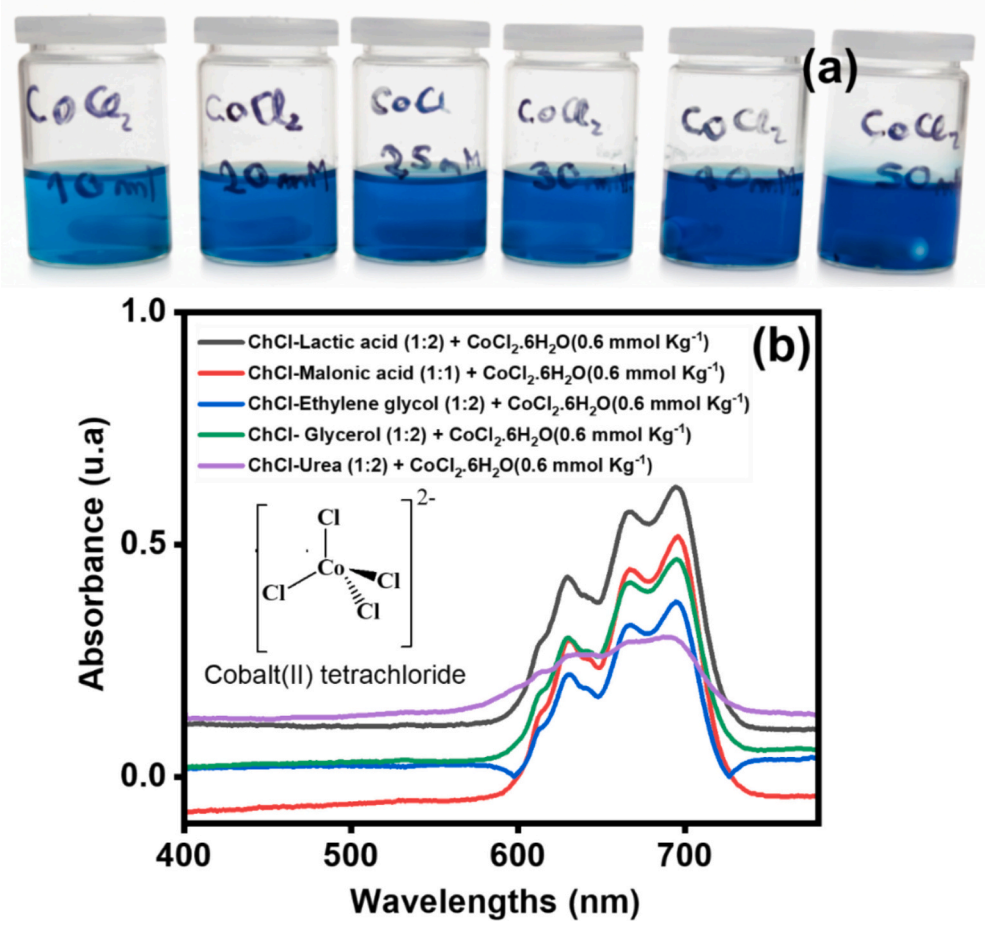

Fig. 3. Dissolution of cobalt (II) chloride hexahydrate in these DESs: **(a)** color observed and **(b)** UV/vis spectra.

weak-field ligand according to the spectrochemical series unlike the hydrogen-bond-donating ligands present in these deep eutectic solvents. Because carboxylates (lactate and malonate), glycerol, ethylene glycol, and urea are generally larger and bulkier than chloride ions. The large size of hydrogen-bond-donating ligands limits the ability to coordinate efficiently around the cobalt metal center.

Furthermore, although these ligands have a stronger field than Cl^-, their ability to stabilize the cobalt complex may be reduced due to their partial protonation of acidic DESs. Indeed, in acidic DESs, the carboxylate groups ($–COO^-$) of lactate and malonate can be protonated to –COOH, which reduces their complexing power with Co^{2+} [9].

Thus, under these conditions, cobalt (II) tends to preferentially complex with chloride ions to form the $[CoCl_4]^{2-}$ complex, which is more thermodynamically stable and characteristic of a tetrahedral geometry. In order to confirm these results, FTIR spectra were recorded and the results obtained for the choline chloride – lactic acid; choline chloride - glycerol and choline chloride - urea DES in absence and presence of Co^{2+} ions are shown on fig. S4.

We can see on this Fig.S4 FT-IR spectra, when the $CoCl_2.6H_2O$ is added in the DES containing chloride-Lactic acid (1:2), no difference is observed between the FT-IR spectra of DES and FTIR spectra of DES + $CoCl_2.6H_2O$. This result confirms that no complexation reaction between ligands of DES with Co^{2+} or hydrogens bonds donors with Co^{2+} occurs. The same results are obtained when the FTIR spectra were recorded in chloride-glycerol (1:2) and choline chloride-Urea (1:2) DESs.

These results confirm the weak interaction of Co^{2+} with carboxylate, glycerol and urea ligands, supporting the hypothesis of a predominant complexation of Cl^-.

Furthermore, $[CoCl_4]^{2-}$, complexes are known to be stable in acidic and chloride rich medium, with an intense blue color [36].

The mechanism of formation of tetrachlorocobaltate (II) complexes result from the salt dissociation, ligand substitution, and geometric reorganization process. Due to the low free water content of DES, chloride ions become highly competitive ligands toward Co^{2+} ions. The salt dissociates according to the following reaction (3):

$$CoCl_2.6H_2O \rightarrow [Co(H_2O)_6]^{2+} + 2Cl^- \quad (3)$$

In the chloride rich choline chloride based DESs, the coordinated water molecules are progressively replaced by chloride ligands. This ligand substitution changes the coordination geometry of Co^{2+} from an octahedral hydrated complexes to a tetrahedral chloro complexes, thereby modifying the crystal field splitting of the cobalt d orbitals [1,33,36,37,39]. As a result, the wavelengths absorbed in the visible region are altered, giving rise to the characteristic blue coloration associated with d-d electronic transitions of cobalt (II). The blue color therefore provides direct evidence of cobalt speciation and the predominant formation of tetrahedral cobalt species in the eutectic medium, according to the following equilibrium (4):

$$[Co(H_2O)_6]^{2+} + 4Cl^- \rightleftharpoons [CoCl_4]^{2-} + 6H_2O \quad (4)$$

This transformation from octahedral hydrated cobalt (II) complexes to tetrahedral chloro complexes is accompanied by an intense blue coloration.

3.3.2. *Pure salts nickel*

In the case of nickel (II) chloride hexahydrate ($NiCl_2.6H_2O$), the pure deep eutectic solvents are initially colorless at 80 °C. Upon dissolution of

the metal salt in choline chloride – lactic acid (1:2), choline chloride - glycerol (1:2), choline chloride - ethylene glycol (1:2), and choline chloride - urea (1:2) (Fig.4.a), a green coloration appears, characteristic of Ni^{2+} complexes.

This result was supported by the data obtained by UV–vis spectroscopy which exhibits a maximum absorption of around 400 nm to 430 nm, characteristic of green color (Fig.4.b).

However, in chloride-malonic acid (1:1) DES solution exhibits a blue coloration (Fig.5.a) with absorption bands typical of Ni^{2+} ions in the UV–vis spectrum between 650 nm and 750 nm (Fig.5.b).

These color differences likely reflect distinct coordination modes of the Ni^{2+} cation, depending on the nature of the deep eutectic solvent. The green coloration can be associated with d-d electronic transitions typical of octahedrally coordinated Ni(II) ions bound to organic molecules of DESs molecules, whereas the blue coloration likely arises from tetrahedral coordination of Ni^{2+} [2,40]. When the hydrogen bond donor is not malonic acid, the presence of a band between 400 nm and 430 nm characteristic of octahedral Ni^{2+} complexes indicates coordination of these molecules (lactic acid, glycerol, ethylene glycol or urea) to the metal center, forming octahedral coordination complexes with Ni(II) ions. This is consistent with the octahedral geometry, as the intensity of the first band between 400 and 430 nm exceeds that of the band observed between 650 nm and 750 nm, indicating a strong preference for coordination with HBD ligands. The shoulders observed at 650 and 750 nm can be attributed to the formation of tetrahedral $[NiCl_4]^{2-}$ complexes, which absorb at lower energy an effect previously reported in chloride rich ionic media. These results are in agreement with reported data in the literature [9,13,17,33,40]. Indeed, Wei et al. (2008) and Gu et al. (2011) demonstrated that increasing the Cl^-/Ni^{2+} molar ratio in ionic liquids and DES induces solvatochromic changes due to the progressive formation of Ni(II) complexes, evolving from octahedral $[NiCl_x(HBD)_{6-x}]^{2-x}$ to chlorinated species and ultimately to tetrahedral $[NiCl_4]^{2-}$.

In choline chloride-based DESs, which are intrinsically rich in Cl^-, increasing Ni^{2+} concentration leads to higher UV/Vis absorption intensity, consistent with Gu and Tu [41]. This suggests a Cl^-/Ni^{2+} ratio ranging from 0 to >20 leading to the formation of different species. Thus, in choline chloride-based DES combined with hydrogen bond donors such as lactic acid, ethylene glycol, glycerol or urea, octahedral solvated complexes coexist with chlorinated tetrahedral species absorbing at lower energies (longer wavelengths). However, the dominant species most often corresponds to solvated octahedral complexes because they exhibit the high UV–Vis absorption intensity.

Although HBDs are stronger field ligands than Cl^-, their coordination to Ni^{2+} is weakened by competition with Cl^- and partial protonation of functional groups, which $[NiCl_4]^{2-}$ can be more thermodynamically stable than strong-field octahedral complexes, high Cl^- concentrations favor tetrahedral geometry [42].

UV–Vis bands in Fig.4.a at 650 nm - 750 nm indicates $[NiCl_4]^{2-}$ formation, whereas bands at 400 nm - 430 nm reflect Ni-HBD coordination, confirming the coexistence of multiple Ni^{2+} complexes. This ligand-dependent equilibrium highlights the coordination flexibility of

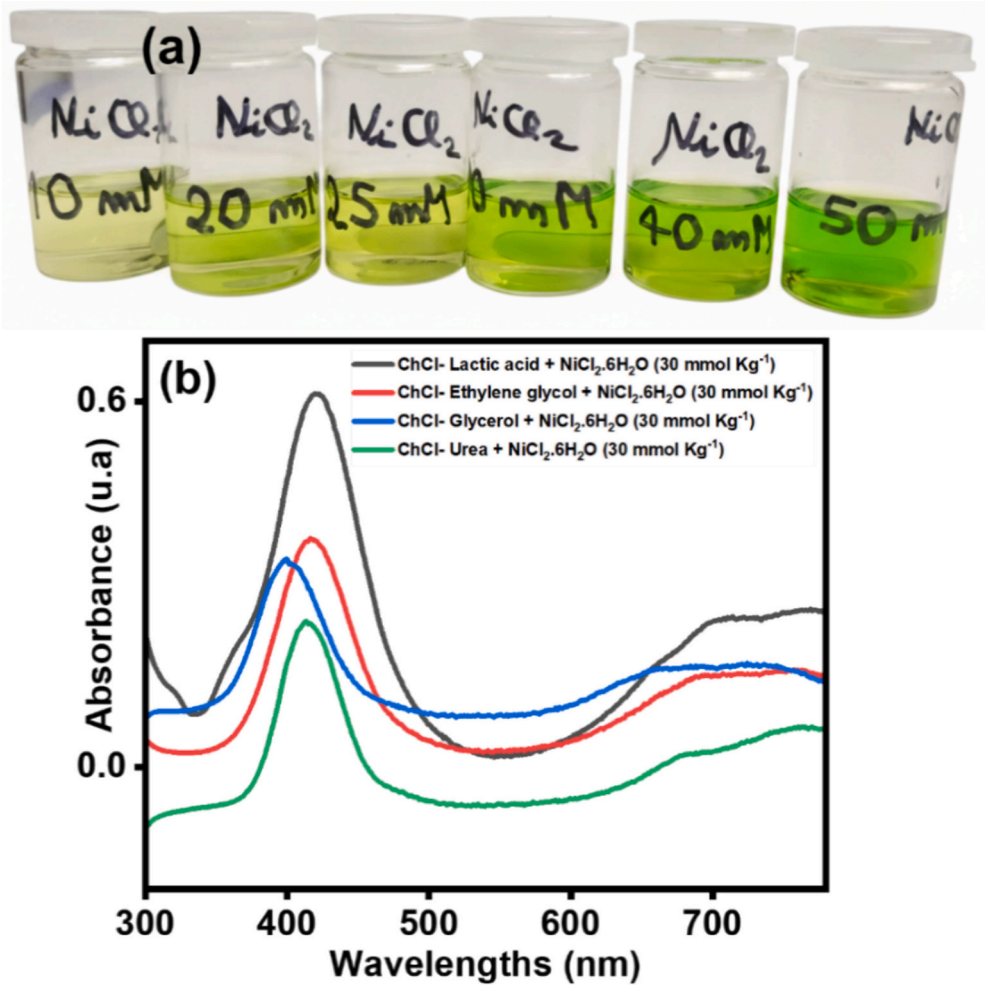

Fig. 4. Dissolution of nickel (II) chloride hexahydrate in chloride-lactic acid (1:2), choline chloride-glycerol (1:2), choline chloride-ethylene glycol (1:2), and choline chloride-urea (1:2) DES (30 mmol Kg^{-1}) DES: **(a)** color observed **(b)** UV/vis spectra.

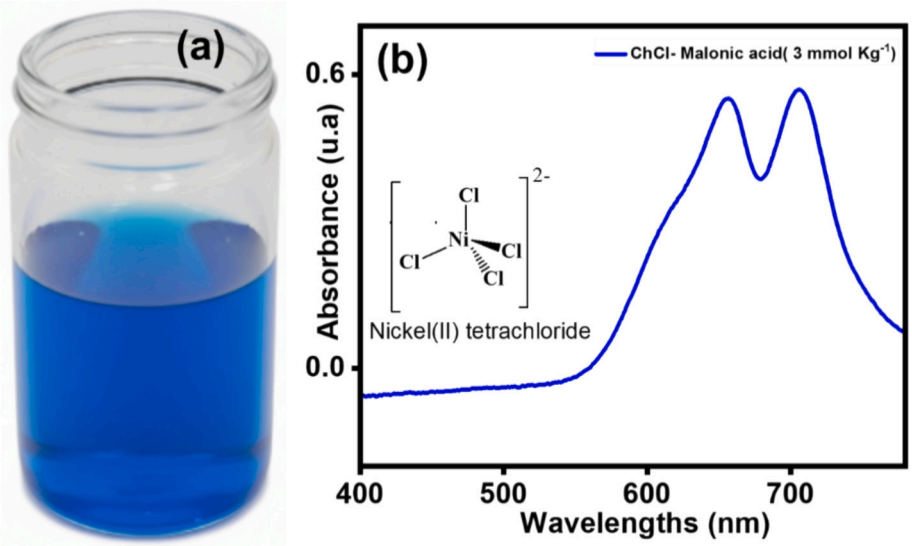

Fig. 5. Dissolution of nickel (II) chloride hexahydrate in chloride- malonic acid (1:1) (3 mmol Kg^{-1}) **(a)** color observed and **(b)** UV/vis spectra.

Ni (II), which may strongly influence metal leaching and recovery processes.

FT-IR spectra of choline chloride-Lactic acid (1:2), choline chloride-glycerol (1:2) and choline chloride-Urea (1:2) DESs before and addition of $NiCl_2.6H_2O$, are shown in fig. S5.

One can't note that significant changes were observed in the characteristic vibrational bands upon nickel addition, indicating weak direct coordination between Ni^{2+} ions and the HBD functional groups. This suggests that Ni^{2+} preferentially complexes with Cl^- ions, forming $[NiCl_4]^{2-}$ species of tetrahedral geometry, while only weak electrostatic interactions occur between Ni^{2+} and the HBD molecules. These results suggest that Ni^{2+} preferentially interacts with chloride ions, forming tetrahedral $[NiCl_4]^{2-}$ complexes, while UV–Visible bands between 400 nm and 430 nm confirm the weakly bound between Ni^{2+} and HBD ligands species (fig.

4.b). The unchanged FT-IR spectra confirms that these interactions are mainly electrostatic rather than coordinative.

These results align with literature reports indicating that Ni(II) favors coordination with chloride ions, followed by monocarboxylic acids, while dicarboxylic acids such as malonic acid can form chelating complexes through both carbonyl groups [1,2,43,44].

According to the Tanabe Sugano diagram for a d^8 electronic configuration, the ground state ($^3A_2g(F)$) of nickel in a octahedral field should have three major spin-allowed transition: $^3A_2g \rightarrow {}^3T_2g(F)$ transition located int the infra-red region, and not recorder because therefore it is therefore out of the range of our spectrometer where the range wavelengths is 280 nm to 780 nm. The second transition is $^3A_2g(F) \rightarrow {}^3T_1g(F)$ in the 600 nm–800 nm range and the third transition in the 350 nm −500 nm range is $^3A_2g(F) \rightarrow {}^3T_1g(P)$ [1,38,45]. These results are summarized in Table 6 for each DES.

The $^3A_2g(F) \rightarrow {}^3T_1g(F)$ transition lies in the region of the spectrum as the peak corresponding to the tetrahedral field species is split, with peaks between 600 nm–800 nm in the DES with Ni^{2+} ion. This is due to spin-orbit coupling that mixes the $^3T_1g(F)$ and $^1Eg(D)$ states [39]. This is due to the high intensity of absorption in octahedral species than tetrahedral field species due to the presence of an inversion center [1].

When the hydrogen bond donor used is dicarboxylic acid such as malonic acid, the two peaks at 658.2 nm and 708.1 nm correspond to the tetrahedral complexes of nickel $[NiCl_4]^{2-}$] (Fig.4b). Using a Tanabe Sugano diagram for a d^8 electronic configuration, one should we would expect three spin allowed transition [1]: $^3T_{1g}(F) \rightarrow {}^3T_{2g}(F)$, $^3T_{1g}(F) \rightarrow {}^3A_{2g}(F)$ and $^3T_{1g}(F) \rightarrow {}^3T_{1g}(P)$. The two peaks observed in the Ni^{2+} spectra are actually correspond one peak of $^3T_1g(F) \rightarrow {}^3T_1g(P)$ transition

Table 6
Spectroscopic data from for Ni^{2+} in DES, including λ_{max} values, observed colors, and corresponding electronic transitions.

DESs	λmax /nm	Intensity	Colors	Electronic transitions
	425.3	strong		
ChCl - La (1:2)	708.3	low		
	764.2	low		
	405.8	strong		$^3A_2g(F) \rightarrow {}^3T_1g(P)$
ChCl - Gly (1:2)	680	low		
	746.7	low		$^3A_2g(F) \rightarrow {}^3T_1g(F)$
	420.9	strong	green	
ChCl - EG (1:2)	691.4	low		
	760.5	low		
	417.8	strong		
ChCl - Ur (1:2)	680	low		
	753.2	low		
ChCl - Malo (1:1)	685.2	strong	Blue	$^3T_{1g}(F) \rightarrow {}^3T_{1g}(P)$
	708.1			

(Table 6), split into several components due to spin-orbit coupling [1,39]. The two other spins allowed transitions lie outside the energy range accessible by UV/Vis spectroscopy.

The formation mechanism of the tetrachloronickelate (II) complexes, as well as the blue coloration of the solution, may be explained according to the same principle proposed for cobalt in section 3.2.1. The corresponding complexation equilibria can be described by the following eqs. (5),(6):

$$NiCl_2.6H_2O \rightarrow \left[Ni(H_2O)_6\right]^{2+} + 2Cl^- \quad (5)$$

$$\left[Ni(H_2O)_6\right]^{2+} + 4Cl^- \rightleftharpoons [NiCl_4]^{2-} + 6H_2O \quad (6)$$

Furthermore, malonate ions ($C_3H_2O_4{}^{2-}$) in the DES can be form chelates with nickel ions [2], and the relevant chemical reaction equation is as follows (7):

$$Ni^{2+} + C_3H_2O^{2-} \rightarrow [Ni(C_3H_2O_4)] \quad (7)$$

In contrast, the formation of octahedral nickel (II) complexes may be explained by the progressive substitution of coordinated water by HBD derived ligands and chloride ions, according to the following eq. (8) and (9):

$$NiCl_2.6H_2O \rightarrow \left[Ni(H_2O)_6\right]^{2+} + 2Cl^- \quad (8)$$

$$\left[Ni(H_2O)_6\right]^{2+} + xCl^- + (6-x)HBD \rightleftharpoons \left[NiCl_x(HBD)_{6-x}\right]^{2-x} + 6H_2O \quad (9)$$

These results of the metal speciation analysis indicate that, in the same matrix containing Ni^{2+} and Co^{2+} ions, their quantification by UV/Vis could be biased by the significant overlap of their absorption bands in the wavelength range of 650 nm to 780 nm. This spectral interference could lead to errors in the quantification of their concentration.

3.4. Colorimetric dosage of cobalt in $LiCoO_2$ type batteries cathodes

For the determination of cobalt in a Li-ion battery by UV/Visible spectroscopy, a Li-ion battery cathode of the $LiCoO_2$ was used. The choline chloride - lactic acid (1:2) system was used as DES for this study due to its acidic nature and high solubilizing power. This DES can effectively dissolve lithium cobalt oxide owing to the ability of acidic protons to act as good oxygen acceptors, thereby promoting the disruption of the metal oxide lattice [1,13,22].

Calibration curves for cobalt ions were established by UV-spectroscopy at maximum intensity wavelengths of 693.3 nm in the choline chloride - lactic acid (1:2) DES medium and represented in the following fig. S6.

One can observe a straight line of the representation of the absorbance upon Co^{2+} concentration. This result confirms that the beer Lambert law is valid in this DES (eq. 2). The explanation of this calibration curve permits the determination of cobalt amount in the three samples of $LiCoO_2$, and the results obtained are summarized in Table 7.

It appears in this table that the amount of the X1 sample is close to 56 ± 0.7 mg L^{-1}. For samples X2 and X3 the presented results show cobalt (II) concentrations of 46.48 ± 0.7 mg L^{-1} and 47.17 ± 2 mg L^{-1} for samples X2 et X3, respectively, as determined by UV–visible spectrophotometric analysis. To confirm these results, the same samples were additionally analyzed using ICP-OES.

The ICP-OES results, summarized in Table 8, allow us to assess the analytical accuracy and provide validation for the spectrophotometric method employed.

The results obtained from the analysis of samples X1, X2, and X3 revealed the presence of two major metals originating from the cathode: lithium and cobalt. The cobalt concentrations measured by ICP-OES in samples X1, X2, and X3 were 57.67 ± 1.2 mg L^{-1}; 47.20 ± 0.9 mg L^{-1} and 47.67 ± 0.7 mg L^{-1}, respectively. These values are very close to those obtained by UV/Visible spectroscopy.

The strong agreement between the two sets of results confirms the accuracy and reliability of the UV/visible method for cobalt determination in DES media.

Furthermore, the calibration curves established for cobalt in DES media confirm the feasibility of accurately determining metals exhibiting characteristic absorption in the UV–visible region. This experimental consistency demonstrates that UV–visible spectroscopy can serve as rapid, cost-effective, and sufficiently accurate alternative to ICP-OES for transition metal quantification in Li-ion battery cathodes.

These findings open promising routes for the analysis and recovery of valuable metals from end-of-life lithium-ion batteries, within the framework of more environmentally sustainable recycling processes.

4. Conclusion

This work is focused on the chemical speciation of Co^{2+} and Ni^{2+} metal ions and colorimetric determination of Ni^{2+} and Co^{2+} ions in deep eutectic solvent media using UV/Vis spectroscopy.

This study of the speciation of Ni^{2+} and Co^{2+} ion in deep eutectic solvent media supports the idea that complex geometry is not influenced by concentration, but rather the nature of the available ligands. Cobalt (II) shows a marked preference for coordination with chloride ligands (Cl^-), whereas for nickel (II), the predominance of complexes involving hydrogen bond donor (HBD) ligands suggests a preferential interaction between Ni^{2+} and these organic ligands, in partial competition with chloride ligands. However, in the dicarboxylic acid DES, only a single dominant species, a tetrahedral complexes.

Table 7
Quantitative determination of cobalt in an $LiCoO_2$ cathode samples using UV–Visible spectrophotometry.

LCO cathodes samples	Wavelengths (nm)	Absorbance (u.a)	Cobalt concentrations (mmol Kg^{-1})	Cobalt concentrations (mg L^{-1})
X1		0.75	0.82 ± 0.01	56 ± 0.70
X2	693.3	0.62	0.67 ± 0.01	46.48 ± 0.70
X3		0.64	0.69 ± 0.03	47.17 ± 2.01

Table 8
Quantitative determination of cobalt in an LCO cathode sample using ICP-OES.

$LiCoO_2$ cathode samples	Metals	Concentration (mg L^{-1})
X1	Li	5.36 ± 0.3
	Co	57.67 ± 1.2
X2	Li	4.60 ± 0.5
	Co	47.20 ± 0.9
X3	Li	4.51 ± 0.2
	Co	47.67 ± 0.7

The determination of cobalt extracted from Li-ion battery cathodes in the ChCl-Lactic acid (1:2) DES yielded concentrations of 56 ± 0.7 mg L^{-1}, 46.48 ± 0.7 mg L^{-1}, and 47.17 ± 2 mg L^{-1} for samples X3, X4, and X5, respectively. These values are in excellent agreement with those obtained by ICP-OES analysis confirming the accuracy and reliability of UV/Vis colorimetric approach for Co^{2+} determination in DES media.

Overall, these findings demonstrate that the dissolution of transition metal salts and battery Lithium cathode in choline chloride - based green solvents enables both efficient solubilization and colorimetric quantification using UV/Visible spectroscopy. Furthermore, the speciation analysis highlights that Ni^{2+} and Co^{2+} exhibit distinct coordination preferences in DES media, suggesting the possibility of selective separation and recovery of cobalt and nickel from mixed metal systems, an important step toward the sustainable recycling of Li-ion battery materials.

CRediT authorship contribution statement

Ali Iname: Writing – original draft, Software, Methodology, Formal analysis, Data curation. **Véronique Vitry:** Writing – review & editing, Supervision, Project administration, Funding acquisition, Conceptualization. **Issa Tapsoba:** Writing – review & editing, Supervision, Project administration, Funding acquisition, Conceptualization.

Declaration of competing interest

The authors declare that they have no known competing financial interests or personal relationships that could have appeared to influence the work reported in this paper.

Acknowledgments

This work was financially supported by ARES-CCD and the authors would like to thank Materia Nova Research Center in Mons (Belgium) for ICP-OES analysis.

Appendix A. Supplementary data

Supplementary data to this article can be found online at https://doi.org/10.1016/j.molliq.2026.129750.

Data availability

No data was used for the research described in the article.

References

[1] J.T.M. Amphlett, M.D. Ogden, W. Yang, S. Choi, Probing Ni2+ and Co2+ speciation in carboxylic acid based deep eutectic solvents using UV/Vis and FT-IR spectroscopy, J. Mol. Liq. 318 (2020) 114217, https://doi.org/10.1016/j.molliq.2020.114217.

[2] Y. Bao, D. Ju, L. Jiang, et al., Recovery of Li, Ni, Co, and Mn from cathode mass of spent lithium-ion batteries by deep eutectic solvent-based pressurized leaching, J. Sustain. Metall. (2025), https://doi.org/10.1007/s40831-025-01229-6.

[3] S. Zheng, S. Xu, Z. Wang, et al., Efficient leaching of valuable metals from spent lithium-ion batteries using green deep eutectic solvents: process optimization, mechanistic analysis, and environmental impact assessment, J. Clean. Prod. 480 (2024) 144128, https://doi.org/10.1016/j.jclepro.2024.144128.

[4] M. Grohol, C. Veeh, Study on the Critical Raw Materials for the EU 2023: Final Report, Publications Office of the European Union, 2023.

[5] M. Li, C. Liu, A. Ding, C. Xiao, A review on the extraction and recovery of critical metals using molten salt electrolysis, J. Environ. Chem. Eng. 11 (2023) 109746, https://doi.org/10.1016/j.jece.2023.109746.

[6] N. Akhmetov, A. Manakhov, A.S. Al-Qasim, Li-ion battery cathode recycling: an emerging response to growing metal demand and accumulating battery waste, Electronics 12 (2023) 1152, https://doi.org/10.3390/electronics12051152.

[7] J. Zou, R. Zhang, Y. Huang, et al., High efficiency leaching of black powder from spent lithium-ion battery by ternary deep eutectic solvent and recovery of metals by precipitation and electrodeposition, Sep. Purif. Technol. 364 (2025) 132438, https://doi.org/10.1016/j.seppur.2025.132438.

[8] S. Wellens, B. Thijs, K. Binnemans, An environmentally friendlier approach to hydrometallurgy: highly selective separation of cobalt from nickel by solvent extraction with undiluted phosphonium ionic liquids, Green Chem. 14 (2012) 1657, https://doi.org/10.1039/c2gc35246j.

[9] Y. Lyu, J.A. Yuwono, Y. Fan, et al., Selective extraction of critical metals from spent Li-ion battery cathode: cation–anion coordination and anti-solvent crystallization, Adv. Mater. 36 (2024) 2312551, https://doi.org/10.1002/adma.202312551.

[10] K.A. Omar, R. Sadeghi, Physicochemical properties of deep eutectic solvents: a review, J. Mol. Liq. 360 (2022) 119524, https://doi.org/10.1016/j.molliq.2022.119524.

[11] D.L. Thompson, I.M. Pateli, C. Lei, et al., Separation of nickel from cobalt and manganese in lithium ion batteries using deep eutectic solvents, Green Chem. 24 (2022) 4877–4886, https://doi.org/10.1039/D2GC00606E.

[12] M.K. Tran, M.-T.F. Rodrigues, K. Kato, et al., Deep eutectic solvents for cathode recycling of Li-ion batteries, Nat. Energy 4 (2019) 339–345, https://doi.org/10.1038/s41560-019-0368-4.

[13] I.M. Pateli, D. Thompson, S.S.M. Alabdullah, et al., The effect of pH and hydrogen bond donor on the dissolution of metal oxides in deep eutectic solvents, Green Chem. 22 (2020) 5476–5486, https://doi.org/10.1039/D0GC02023K.

[14] N. Altunay, A. Elik, R. Gürkan, Monitoring of some trace metals in honeys by flame atomic absorption spectrometry after ultrasound assisted-dispersive liquid liquid microextraction using natural deep eutectic solvent, Microchem. J. 147 (2019) 49–59, https://doi.org/10.1016/j.microc.2019.03.003.

[15] E. Bağda, H. Altundağ, M. Soylak, Highly simple deep eutectic solvent extraction of manganese in vegetable samples prior to its ICP-OES analysis, Biol. Trace Elem. Res. 179 (2017) 334–339, https://doi.org/10.1007/s12011-017-0967-5.

[16] E. Habibi, K. Ghanemi, M. Fallah-Mehrjardi, A. Dadolahi-Sohrab, A novel digestion method based on a choline chloride–oxalic acid deep eutectic solvent for determining cu, Fe, and Zn in fish samples, Anal. Chim. Acta 762 (2013) 61–67, https://doi.org/10.1016/j.aca.2012.11.054.

[17] J.M. Hartley, C.-M. Ip, G.C.H. Forrest, et al., EXAFS study into the speciation of metal salts dissolved in ionic liquids and deep eutectic solvents, Inorg. Chem. 53 (2014) 6280–6288, https://doi.org/10.1021/ic500824r.

[18] I.N. Perera, G.S. Dobhal, J.M. Pringle, et al., A case study using spectroscopy and computational modelling for co speciation in a deep eutectic solvent, Phys. Chem. Chem. Phys. 26 (2024) 21087–21098, https://doi.org/10.1039/D4CP01471E.

[19] S.P. Ijardar, V. Singh, R.L. Gardas, Revisiting the physicochemical properties and applications of deep eutectic solvents, Molecules 27 (2022) 1368, https://doi.org/10.3390/molecules27041368.

[20] F.G. Calvo-Flores, C. Mingorance-Sánchez, Deep eutectic solvents and multicomponent reactions: two convergent items to green chemistry strategies, ChemistryOpen 10 (2021) 815–829, https://doi.org/10.1002/open.202100137.

[21] N. Cao, Y. Zhang, L. Chen, et al., Priority recovery of lithium and effective leaching of nickel and cobalt from spent lithium-ion battery, Trans. Nonferrous Metals Soc. China 32 (2022) 1677–1690, https://doi.org/10.1016/S1003-6326(22)65902-8.

[22] R. Morina, D. Callegari, D. Merli, et al., Cathode active material recycling from spent Lithium batteries: a green (circular) approach based on deep eutectic solvents, ChemSusChem 15 (2022) e202102080, https://doi.org/10.1002/cssc.202102080.

[23] H. Qin, X. Hu, J. Wang, et al., Overview of acidic deep eutectic solvents on synthesis, properties and applications, Green Energy Environ. 5 (2020) 8–21, https://doi.org/10.1016/j.gee.2019.03.002.

[24] A.L. Sazali, N. AlMasoud, S.K. Amran, et al., Physicochemical and thermal characteristics of choline chloride-based deep eutectic solvents, Chemosphere 338 (2023) 139485, https://doi.org/10.1016/j.chemosphere.2023.139485.

[25] D. Yue, Y. Jia, Y. Yao, et al., Structure and electrochemical behavior of ionic liquid analogue based on choline chloride and urea, Electrochim. Acta 65 (2012) 30–36, https://doi.org/10.1016/j.electacta.2012.01.003.

[26] Y. Li, Y. Li, H. Li, et al., Insights into the tribological behavior of choline chloride—urea and choline chloride—thiourea deep eutectic solvents, Friction 11 (2023) 76–92, https://doi.org/10.1007/s40544-021-0575-4.

[27] N. Delgado-Mellado, M. Larriba, P. Navarro, et al., Thermal stability of choline chloride deep eutectic solvents by TGA/FTIR-ATR analysis, J. Mol. Liq. 260 (2018) 37–43, https://doi.org/10.1016/j.molliq.2018.03.076.

[28] C. Cao, Z. Yuan, H. Liu, et al., Lactic-acid-based deep eutectic solvent for sustainable recovery of critical metals from spent lithium-ion batteries under mild conditions, J. Clean. Prod. 512 (2025) 145460, https://doi.org/10.1016/j.jclepro.2025.145460.

[29] A.P. Abbott, D. Boothby, G. Capper, et al., Deep eutectic solvents formed between choline chloride and carboxylic acids: versatile alternatives to ionic liquids, J. Am. Chem. Soc. 126 (2004) 9142–9147, https://doi.org/10.1021/ja048266j.

[30] B. Lu, R. Du, G. Wang, et al., High-efficiency leaching of valuable metals from waste Li-ion batteries using deep eutectic solvents, Environ. Res. 212 (2022) 113286, https://doi.org/10.1016/j.envres.2022.113286.

[31] X. Chang, M. Fan, C. Gu, et al., Selective extraction of transition metals from spent $LiNi_xCo_yMn_{1-x-y}O_2$ cathode via regulation of coordination environment, Angew. Chem. Int. Ed. 61 (2022) e202202558, https://doi.org/10.1002/anie.202202558.

[32] J. Cheng, C. Zheng, K. Xu, et al., Sequential separation of critical metals from lithium-ion batteries based on deep eutectic solvent and electrodeposition, J. Hazard. Mater. 465 (2024) 133157, https://doi.org/10.1016/j.jhazmat.2023.133157.

[33] S. Aberdeen, R.I. Foster, S. Choi, Nickel and cobalt separation via speciation using deep eutectic solvent-based ion exchange, Sep. Purif. Technol. 375 (2025) 133833, https://doi.org/10.1016/j.seppur.2025.133833.

[34] A. Can, İ. Özlüsoylu, P. Antov, S.H. Lee, Choline chloride-based deep eutectic solvent-treated wood, Forests 14 (2023) 569, https://doi.org/10.3390/f14030569.

[35] M. Bučko, J. Bajat, A review of the electrochemical corrosion of metals in choline chloride based deep eutectic solvents: review paper, J Electrochem Sci Eng. (2021), https://doi.org/10.5599/jese.1135.

[36] A.Y.M. Al-Murshedi, A. Al-Yasari, H.F. Alesary, H.K. Ismail, Electrochemical fabrication of cobalt films in a choline chloride–ethylene glycol deep eutectic solvent containing water, Chem. Pap. 74 (2020) 699–709, https://doi.org/10.1007/s11696-019-01025-z.

[37] J. Estager, J.D. Holbrey, M. Swadźba-Kwaśny, Halometallate ionic liquids – revisited, Chem. Soc. Rev. 43 (2014) 847–886, https://doi.org/10.1039/C3CS60310E.

[38] P. Rybka, M. Regel-Rosocka, Nickel(II) and cobalt(II) extraction from chloride solutions with quaternary phosphonium salts, Sep. Sci. Technol. 47 (2012) 1296–1302, https://doi.org/10.1080/01496395.2012.672532.

[39] S. Iuchi, S. Sakaki, Spin–orbit coupling in a model Hamiltonian for d–d excited states of Ni2+ ion aqueous solution, Chem. Phys. Lett. 485 (2010) 114–118, https://doi.org/10.1016/j.cplett.2009.12.039.

[40] X. Wei, L. Yu, D. Wang, et al., Thermo-solvatochromism of chloro-nickel complexes in 1-hydroxyalkyl-3-methyl-imidazolium cation based ionic liquids, Green Chem. 10 (2008) 296, https://doi.org/10.1039/b715763k.

[41] C.-D. Gu, J.-P. Tu, Thermochromic behavior of chloro-nickel(II) in deep eutectic solvents and their application in thermochromic composite films, RSC Adv. 1 (2011) 1220, https://doi.org/10.1039/c1ra00345c.

[42] D.F.C. Morris, G.L. Reed, E.L. Short, et al., Nickel (II) chloride complexes in aqueous solution, J. Inorg. Nucl. Chem. 27 (1965) 377–382, https://doi.org/10.1016/0022-1902(65)80355-4.

[43] R. Golmohammadzadeh, Z. Dimachki, W. Bryant, et al., Removal of polyvinylidene fluoride binder and other organics for enhancing the leaching efficiency of lithium and cobalt from black mass, J. Environ. Manag. 343 (2023) 118205, https://doi.org/10.1016/j.jenvman.2023.118205.

[44] E.L. Smith, A.P. Abbott, K.S. Ryder, Deep eutectic solvents (DESs) and their applications, Chem. Rev. 114 (2014) 11060–11082, https://doi.org/10.1021/cr300162p.

[45] W. Liu, A. Migdisov, A. Williams-Jones, The stability of aqueous nickel(II) chloride complexes in hydrothermal solutions: results of UV–visible spectroscopic experiments, Geochim. Cosmochim. Acta 94 (2012) 276–290, https://doi.org/10.1016/j.gca.2012.04.055.